

DETC2012-70391

ON THE DESIGN OF A RECUMBENT BICYCLE WITH A PERSPECTIVE ON HANDLING QUALITIES

A. L. Schwab*
J.D.G. Kooijman

Laboratory for Engineering Mechanics
Delft University of Technology
Mekelweg 2, NL-2628 CD Delft, The Netherlands
e-mail: a.l.schwab@tudelft.nl

J. Nieuwendijk

Otto Bock Healthcare Products GmbH
Kaiserstraße 39
1070 Vienna, Austria

ABSTRACT

A novel approach to bicycle design for handling qualities is presented. The design method is introduced through a case study in which a new front-wheel drive recumbent bicycle is developed. Since there exists no proper definition nor assessment for bicycle handling qualities, design process is based on comparing the uncontrolled dynamics of the new concepts to an existing design, known to handle well. A prototype was built and road test were conducted to compare the handling before being taken into production. The new design shows comparable handling.

INTRODUCTION

An important aspect in bicycle design is handling quality. Unfortunately, handling qualities of a bicycle are not well defined and mostly rely on subjective rider test trials [1]. Some more experience on handling is available for motorcycles, for a recent overview see Popov *et al.* [2]. However, for motorcycles the main issues concern handling at moderate to high speed, which is not the issue for bicycles. For bicycling low speed is of interest, that is in a forward speed range of 0 to 20 km/h. The common practice in the design process of bicycles is to use manufacturer experience and the trial and error method to come to new designs. This evolutionary process is lengthy and cumbersome, and usually leads to suboptimal designs. The aim here is to design bicycles for specific handling qualities.

A proper definition of handling qualities involves the dynamics and control of the complete system: bicycle plus rider. A recent upheaval in bicycle research [3, 4, 5, 6] focuses mainly on the bicycle whereas still little is known about the rider. Some initial work has been done in the 70's on bicycle rider model identification by Van Lunteren and Stassen [7], but these results are limited and inconclusive. A recent paper by Hess *et al.* [8] focusses on control models for the bicycle rider, for which unfortunately no experimental validation is available yet. One conjecture is that handling qualities are closely related to the dynamics of the uncontrolled vehicle [6]. Moreover, recent experimental observations on bicycle rider motions [9, 10] show that the rider does not really move relative to the bicycle and thus that a rigidly attached rider could be a valid way to model the uncontrolled system. That is the approach we will use here. Starting from an existing design with good handling qualities, as perceived by experienced riders, the uncontrolled stability of the bicycle-rider combination is determined with a computer model. The new design will be made such that it matches the open loop stability of the existing one in the operational forward speed range. As a case study the design of a new front-wheel drive recumbent bicycle for the firm Raptobike [11] is presented. Note that on a recumbent bicycle the rider is not able to move relative to the rear frame, this makes the applied rigid rider model approach even more valid.

The paper is organized as follows. After this introduction the design problem is stated. Next the methods are explained.

*Address all correspondence to this author.



FIGURE 1. Raptobike Lowracer recumbant bicycle, existing design of a front drive recumbant bicycle. To accommodate variable size riders the drive train in front of the head tube can be extended, as indicated by the arrows.



FIGURE 2. Raptobike Midracer recumbant bicycle, new design of a front drive recumbant bicycle. To accommodate variable size riders the rear frame tube between the rear axle and the head tube can be extended, as indicated by the arrows, keeping the drive train length unchanged. Shown is the short version.

Then the results are shown and discussed. The paper ends with some conclusions.

DESIGN PROBLEM

The firm Raptobike [11] produces recumbent bicycles and has been successful with the design of the Lowracer, see Figure 1. This recumbent bicycle has specific characteristics: a long wheel base, low rider position, and front wheel drive. It is known for its good handling qualities. One problem of this front drive concept is that the drive train (chain length) has to be adjusted to accommodate riders of different size. The new concept, called Midracer, solves this problem by having the length adjustment for the rider in the rear frame between the head tube and the rear axle. The short version of the Midracer is shown in Figure 2. An additional design change is the use of equal sized wheels and a higher rider position compared to that of the Lowracer.

However, the proposed length adjustment in the Midracer at the rear frame between the rear axle and the head tube, introduces

a change in the steering geometry. Extension of the rear frame steepens the steer axis and reduces the trail. Steer axis tilt and trail are known to have a significant effect on the dynamics and stability of the bicycle. But so have the mass distribution of the individual bodies and the wheel base [6]. Moreover, in general the short version will be driven by a lighter rider compared to the long version. In this design study the Midracer is considered in two configurations: short and long, with corresponding light and heavy riders.

The design problem is to design the Midracer for the two configurations in such a way that it has comparable handling qualities to that of the existing Lowracer model.

METHOD

Due to the lack of a rider model the conjuncture that handling qualities are closely related to the dynamics of the uncontrolled vehicle [6] will be used. The starting point is the existing model which is known for its good handling qualities. Within the design constraints, the new model parameters are then determined by nonlinear optimization such that the new model shows identical uncontrolled dynamics as the existing one. The new model is built, and handling qualities are accessed by driving tests.

Bicycle Model

The basic bicycle model used is the so-called Whipple model [12], which was recently benchmarked [3]. The model, *see* Figure 3, consists of four rigid bodies connected by revolute joints. The contact between the knife-edged wheels and the flat level surface is modelled by holonomic constraints in the normal direction, prescribing the wheels to touch the surface, and by non-holonomic constraints in the longitudinal and lateral directions, prescribing zero longitudinal and lateral slip. In this model, it is assumed that the rider is rigidly attached to the rear frame and has no hands on the handlebar. The resulting non-holonomic mechanical model has three velocity degrees of freedom: forward speed v , lean rate $\dot{\phi}$ and steering rate $\dot{\delta}$.

For the lateral stability analysis, the linearized equations of motion for small perturbations about the upright steady forward motion are considered. These linearized equations of motion are fully described in [3]. They are expressed in terms of small changes in the lateral degrees of freedom (the rear frame lean angle, ϕ , and the steering angle, δ) from the upright straight-ahead configuration $(\phi, \delta) = (0, 0)$, at a forward speed v , and have the form

$$\mathbf{M}\ddot{\mathbf{q}} + v\mathbf{C}_1\dot{\mathbf{q}} + [g\mathbf{K}_0 + v^2\mathbf{K}_2]\mathbf{q} = \mathbf{f}, \quad (1)$$

where the time-varying variables are $\mathbf{q} = [\phi, \delta]^T$ and the lean and steering torques are $\mathbf{f} = [T_\phi, T_\delta]^T$. The coefficients in this equa-

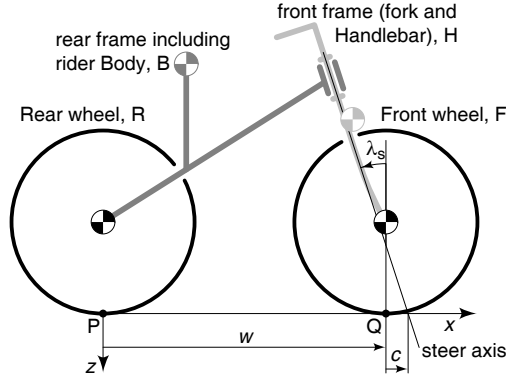


FIGURE 3. The Whipple bicycle model: four rigid bodies (rear wheel R, rear frame B, front handlebar assembly H, front wheel F) connected by three revolute joints (rear hub, steering axis, front hub), together with the wheelbase w , head angle λ_s , and trail c .

tion are: a constant symmetric mass matrix, \mathbf{M} , a damping-like (there is no real damping) matrix, $v\mathbf{C}_1$, which is linear in the forward speed v , and a stiffness matrix which is the sum of a constant symmetric part, $g\mathbf{K}_0$, and a part, $v^2\mathbf{K}_2$, which is quadratic in the forward speed. The forces on the right-hand side, \mathbf{f} , are the applied forces which are energetically dual to the degrees of freedom \mathbf{q} . In the upright straight-ahead configuration, the linearized equation of motion for the forward motion is decoupled from the linearized equations of motion of the lateral motions and simply reads $\dot{v} = 0$.

The entries in the constant coefficient matrices \mathbf{M} , \mathbf{C}_1 , \mathbf{K}_0 and \mathbf{K}_2 can be calculated from a non-minimal set of 25 bicycle parameters as described in [3]. A procedure for measuring these parameters for a real bicycle is described in [13, 10] whereas measured values for the Raptobike Lowracer recumbent bicycle, which is used in this design study, are listed in Table 1. Then, with the coefficient matrices the characteristic equation,

$$\det(\mathbf{M}\lambda^2 + v\mathbf{C}_1\lambda + g\mathbf{K}_0 + v^2\mathbf{K}_2) = 0, \quad (2)$$

can be formed and the eigenvalues, λ , which describe the lateral dynamics as exponential solutions of the form $\mathbf{q} = \mathbf{q}_0 \exp(\lambda t)$, can be calculated. In principle, there are up to four eigenmodes, where oscillatory eigenmodes come in pairs. Two are significant and are traditionally called the *capsize* mode and the *weave* mode, see Figure 4. The capsize mode corresponds to a real eigenvalue with an eigenvector dominated by lean: when unstable, the bicycle follows a spiralling path with increasing curvature until it falls. The weave mode is an oscillatory motion in which the bicycle sways about the heading direction. The third remaining eigenmode is the overall stable *castering* mode, like in a trailing caster wheel, which corresponds to a large negative real eigenvalue with an eigenvector dominated by steering. At

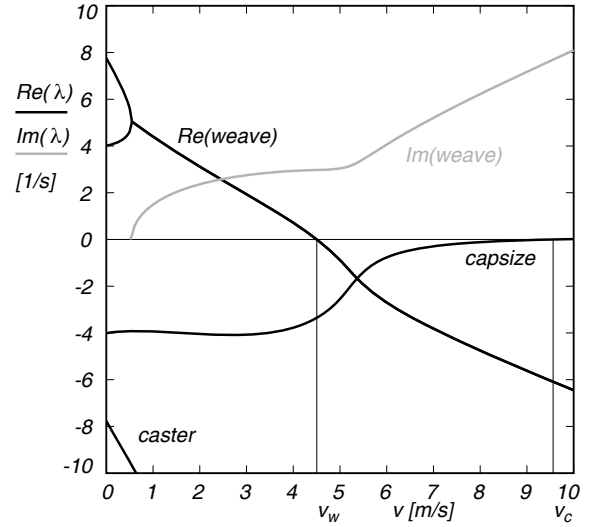


FIGURE 4. Eigenvalues λ from the linearized stability analysis for the Lowracer recumbent bicycle from figure 1 and table 1, where black lines correspond to the real parts of the eigenvalues and the gray line corresponds to the imaginary part of the eigenvalues in the forward speed range of $0 < v < 10$ m/s. The self stable speed range for the Lowracer recumbent bicycle is between the weave speed $v_w \approx 4.5$ m/s and the capsize speed $v_c \approx 9.6$ m/s.

near-zero speeds, typically $0 < v < 0.5$ m/s, there are two pairs of real eigenvalues. Each pair consists of a positive and a negative eigenvalue and corresponds to an inverted-pendulum-like falling of the bicycle. The positive root in each pair corresponds to falling, whereas the negative root corresponds to a righting motion. For $v = 0$, these two are related by a time reversal of the motion. When speed is increased, two real eigenvalues coalesce and then split to form a complex conjugate pair; this is where the oscillatory weave motion emerges. At first, this motion is unstable, but at $v = v_w \approx 4.5$ m/s, the weave speed, these eigenvalues cross the imaginary axis at a Hopf bifurcation and this mode becomes stable. At a higher speed, the capsize eigenvalue crosses the origin at a pitchfork bifurcation at $v = v_c \approx 9.6$ m/s, the capsize speed, and the bicycle becomes mildly unstable. The speed range for which the uncontrolled bicycle shows asymptotically stable behaviour, with all eigenvalues having negative real parts, is $v_w < v < v_c$. But, with the capsize instability being so mild, the bicycle is stable in practice for all speeds above the weave speed.

Optimization

The objective is to find a design for the Midracer recumbent bicycle which, in both short and long version, has identical uncontrolled dynamics when compared to the existing Lowracer recumbent bicycle. For the new Midracer design there are a num-

ber of design constraints like the wheel size, frame size, and rider mass and position, such that the remaining free design parameters are the head angle (steer axis tilt) and the trail. The length adjustment in the Midracer changes the steering geometry. Extension of the rear frame steepens the steering axis and reduces the trail. For the Midracer design, as shown in Figure 2 and Table 2, the sensitivities for the headangle λ_s and the trail c for changes in the wheelbase w are: $\partial\lambda_s/\partial w \approx 15^\circ/\text{m}$ and $\partial c/\partial w \approx -0.1 \text{ m/m}$.

There are various ways to quantify the objective “show identical uncontrolled dynamics”. With only a limited number of free design parameters, here the head angle and the trail, it is in general not possible for all four eigenvalues to be identical in the complete forward speed range of $0 < v < 10 \text{ m/s}$. However, the weave speed plays an important roll in the transition from unstable to stable lateral motions. Therefore, the objective here is quantified by the weave speed for the Midracer, in both short and long version, to be the same as for the Lowracer. This objective can be formulated as a nonlinear optimization problem with the to be minimized objective function,

$$J_{min} = (v_{ws} - \bar{v}_w)^2 + (v_{wl} - \bar{v}_w)^2, \quad (3)$$

with the weave speeds for: Lowracer \bar{v}_w , Midracer short v_{ws} , and Midracer long v_{wl} . The free parameters in the optimization are for the Midracer short version the head angle λ_s and the trail c . The values for the Midracer long version follow directly from the Midracer short geometry and the change in steering geometry due to frame extension. The long version has to accommodate a larger person. This results in the following Midracer basic differences: wheelbase short 1.1 m and long 1.3 m, rider cm position short (0.6, 0.8) m and long (0.7, 0.8) m, and rider mass short 60 kg and long 80 kg, see also Tables 2 and 3. The optimization is done in Matlab with the help of `fminsearch`.

RESULTS

After optimization a new design for the Midracer short and long was found which have nearly identical weave speed as the Lowracer model, see Figure 5. The optimized head angle and trail for the Midracer short version are $\lambda_s = 72^\circ$ and $c = 0.049 \text{ m}$. The Midracer long version, with an extended wheelbase of 1.3 m, then has a head angle of $\lambda_s = 74.6^\circ$ and a trail of $c = 0.034 \text{ m}$, see Tables 2 and 3. Not only are the weave speeds nearly identical, but both Midracer designs show close related uncontrolled dynamics around the weave speed to the existing Lowracer. Also the Midracer short and long version uncontrolled dynamics is almost identical. The only visible difference is in the eigenvalues of the caster mode, which is very stable and from a handling perspective therefore of no interest. Overall, compared to the Lowracer, the Midracer the weave frequency is somewhat lower

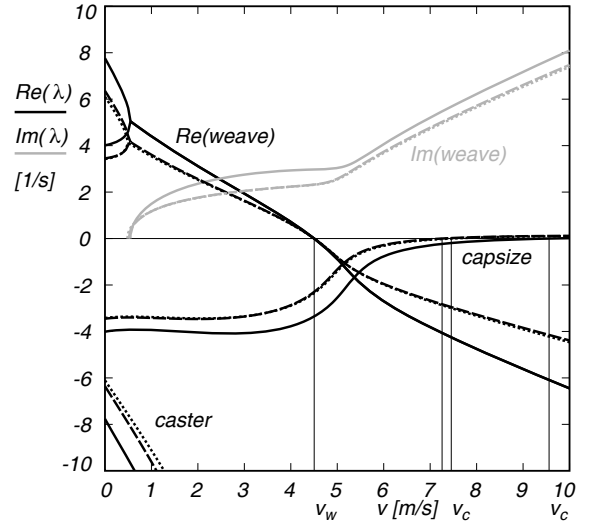


FIGURE 5. Eigenvalues λ from the linearized stability analysis for three Raptobike recumbent bicycles: the original Lowracer (solid lines), the new Midracer in the short version (dashed lines) and the long version (dotted lines), in the forward speed range of $0 < v < 10 \text{ m/s}$. Black lines correspond to the real part of the eigenvalues and gray lines correspond to the imaginary part of the eigenvalues. All three bicycles have the same weave speed $v_w \approx 4.5 \text{ m/s}$. The capsize speed for the three bicycles are different: Lowracer $v_c \approx 9.6 \text{ m/s}$, Midracer short version $v_c \approx 7.3 \text{ m/s}$, and Midracer long version $v_c \approx 7.5 \text{ m/s}$.

and absolute values of real part of the eigenvalues too. This last difference can be attributed to the Midracer higher rider position.

Finally, a prototype of the Midracer was built and tested by experienced riders, both short and long, where the handling showed to be comparable to the existing Lowracer model. The Midracer is now in production.

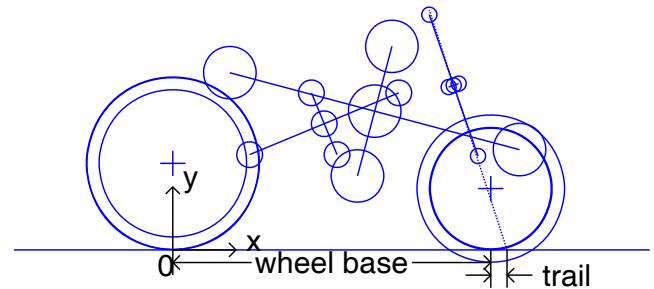
CONCLUSIONS

Based on the conjecture that the handling qualities of a bicycle are closely related to the dynamics of the uncontrolled vehicle, a new model recumbent bicycle was designed. Theoretically this new model, in both the short and the long version, has nearly identical uncontrolled dynamics in comparison to the existing model. In the performed road tests, the built prototype, also showed comparable handling qualities to the existing model. This may indicate that for bicycles there is a close relationship between uncontrolled dynamics and their perceived handling qualities.

REFERENCES

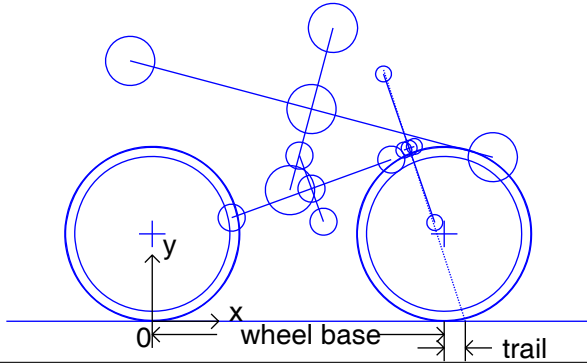
- [1] J.D.G Kooijman and A.L. Schwab. A review on handling aspects in bicycle and motorcycle control. In *Proceedings of the ASME 2011 International Design Engineering Technical Conferences & Computers and Information in Engineering Conference IDETC/CIE 2011 August 28-31, 2011, Washington, DC, USA*. ASME, ASME, August 28–31 2011.
- [2] A. A. Popov, S. Rowell, and J. P. Meijaard. A review on motorcycle and rider modelling for steering control. *Vehicle System Dynamics*, 48:775–792, 2010.
- [3] J. P. Meijaard, Jim M. Papadopoulos, Andy Ruina, and A. L. Schwab. Linearized dynamics equations for the balance and steer of a bicycle: a benchmark and review. *Proceedings of the Royal Society A*, 463:1955–1982, 2007.
- [4] P. Basu-Mandal, A. Chatterjee, and J.M. Papadopoulos. Hands-free circular motions of a benchmark bicycle. *Proceedings of the Royal Society A*, 463:1983–2003, 2007.
- [5] R. S. Sharp. On the stability and control of the bicycle. *Applied Mechanics Reviews*, 61, November, 24 pp. 2008.
- [6] J. D. G. Kooijman, J. P. Meijaard, Jim P. Papadopoulos, Andy Ruina, and A. L. Schwab. A bicycle can be self-stable without gyroscopic or caster effects. *Science*, 332:339–342, April 15, 2011.
- [7] A. van Lunteren and H. G. Stassen. On the variance of the bicycle rider’s behavior. In *Proceedings of the 6th Annual Conference on Manual Control*, April 1970.
- [8] R. Hess, J.K. Moore, and M. Hubbard. Modeling the manually controlled bicycle. *Systems, Man and Cybernetics, Part A: Systems and Humans, IEEE Transactions on*, (99):1–13, 2011.
- [9] J. D. G. Kooijman, A. L. Schwab, and J. K. Moore. Some observations on human control of a bicycle. In *Proceedings of the ASME 2009 International Design Engineering Technical Conferences & Computers and Information in Engineering Conference*, DETC2009, Aug 30 – Sep 2, 2009, San Diego, CA, 2009.
- [10] Jason K. Moore, J. D. G. Kooijman, A. L. Schwab, and Mont Hubbard. Rider motion identification during normal bicycling by means of principal component analysis. *Multibody System Dynamics*, 25(2):225–244, 2011.
- [11] <http://www.raptobike.nl/>.
- [12] F. J. W. Whipple. The stability of the motion of a bicycle. *Quarterly Journal of Pure and Applied Mathematics*, 30:312–348, 1899.
- [13] J. D. G. Kooijman, A. L. Schwab, and J. P. Meijaard. Experimental validation of a model of an uncontrolled bicycle. *Multibody System Dynamics*, 19:115–132, 2008.

TABLE 1. Parameters for the Lowracer recumbent bicycle from figure 1. A sketch of the model, drawn to scale, is shown at the top. In this sketch, the mass moments of inertia of the wheels are indicated by their radii of gyration and the mass moments of inertia for the other rigid bodies are depicted by 6-mass balls lined up in pairs in the three principal directions. The mass of every ball is 1/6 of the total mass (the circle at the center represents both a right mass and a left mass hidden behind it). The principal axes are $(1, 2, z)$, where the 1-axis makes an angle α_1 with the x -axis. For the Whipple bicycle model the rear frame and rider are eventually combined into one rigid body.



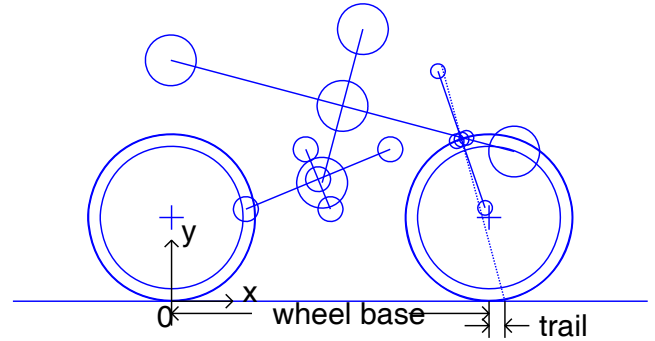
wheel base w	1.26 m	
trail c	0.065 m	
steer axis tilt λ_s	72°	
<i>wheel</i>	<i>rear</i>	<i>front</i>
diameter	0.6858 m	0.4860 m
mass	2 kg	2 kg
moment of inertia I_{xx} & I_{yy}	0.085513 kgm ²	0.085513 kgm ²
moment of inertia I_{zz}	0.171026 kgm ²	0.171026 kgm ²
<i>rear</i>	<i>rear frame</i>	<i>rider</i>
centre of mass (x, y)	(0.6, 0.5) m	(0.8, 0.55) m
mass	10 kg	85 kg
moment of inertia I_{11}	0.058579 kgm ²	2.5 kgm ²
moment of inertia I_{22}	0.341421 kgm ²	10.5 kgm ²
moment of inertia I_{zz}	0.4 kgm ²	12 kgm ²
principal axis angle α_1	22.5°	-14.87°
<i>front</i>	<i>front frame</i>	
centre of mass (x, y)	(1.113, 0.652) m	
mass	2 kg	
moment of inertia I_{11}	0.058579 kgm ²	
moment of inertia I_{22}	0.0000588 kgm ²	
moment of inertia I_{zz}	0.05879 kgm ²	
principal axis angle α_1	19.02°	

TABLE 2. Parameters for the short version of the Midracer recumbent bicycle from figure 2. Shown at the top is a sketch of the model drawn to scale. For further explanation see Table 1.



wheel base w	1.1 m	
trail c	0.049 m	
steer axis tilt λ_s	72°	
<i>wheel</i>		<i>rear</i>
diameter	0.659 m	0.659 m
mass	2 kg	2 kg
moment of inertia I_{xx} & I_{yy}	0.085513 kgm ²	0.085513 kgm ²
moment of inertia I_{zz}	0.171026 kgm ²	0.171026 kgm ²
<i>rear</i>		<i>rear frame</i>
centre of mass (x,y)	(0.6,0.5) m	(0.6,0.8) m
mass	10 kg	60 kg
moment of inertia I_{11}	0.058579 kgm ²	2.5 kgm ²
moment of inertia I_{22}	0.341421 kgm ²	10.5 kgm ²
moment of inertia I_{zz}	0.4 kgm ²	12 kgm ²
principal axis angle α_1	20°	-14.87°
<i>front</i>		<i>front frame</i>
centre of mass (x,y)	(0.968,0.652) m	
mass	2 kg	
moment of inertia I_{11}	0.058579 kgm ²	
moment of inertia I_{22}	0.0000588 kgm ²	
moment of inertia I_{zz}	0.05879 kgm ²	
principal axis angle α_1	19.02°	

TABLE 3. Parameters for the long version of the Midracer recumbent bicycle (see figure 2 for the general layout of the Midracer recumbent bicycle). Shown at the top is a sketch of the model drawn to scale. For further explanation see Table 1.



wheel base w	1.3 m	
trail c	0.034 m	
steer axis tilt λ_s	74.6°	
<i>wheel</i>		<i>rear</i>
diameter	0.6858 m	0.4860 m
mass	2 kg	2 kg
moment of inertia I_{xx} & I_{yy}	0.085513 kgm ²	0.085513 kgm ²
moment of inertia I_{zz}	0.171026 kgm ²	0.171026 kgm ²
<i>rear</i>		<i>rear frame</i>
centre of mass (x,y)	(0.6,0.5) m	(0.7,0.8) m
mass	10 kg	85 kg
moment of inertia I_{11}	0.058579 kgm ²	3.75 kgm ²
moment of inertia I_{22}	0.341421 kgm ²	15.75 kgm ²
moment of inertia I_{zz}	0.4 kgm ²	18 kgm ²
principal axis angle α_1	22.5°	-14.87°
<i>front</i>		<i>front frame</i>
centre of mass (x,y)	(1.188,0.662) m	
mass	2 kg	
moment of inertia I_{11}	0.058579 kgm ²	
moment of inertia I_{22}	0.0000588 kgm ²	
moment of inertia I_{zz}	0.05879 kgm ²	
principal axis angle α_1	19.02°	